Emission rate dependence on the electric field for two trap levels in proton-irradiated *n*-type GaAs

A. V. P. Coelho[1,2,*] and H. Boudinov[1]
[1]*Instituto de Física, Universidade Federal do Rio Grande do Sul, 91501-970 Porto Alegre, RS, Brazil*
[2]*Centro de Excelência em Tecnologia Eletrônica Avançada, 91540-000 Porto Alegre, RS, Brazil*
(Received 4 December 2007; revised manuscript received 7 April 2008; published 16 June 2008)

The electron emission rate dependence on the electric field for two levels in proton bombarded *n*-type GaAs, E1 and E2, was measured at different temperatures. E1 shows an emission enhancement completely described by the phonon-assisted tunneling model. The behavior observed for E2 is described by the sum of a Poole-Frenkel part and a phonon-assisted tunneling contribution. These data support a +/0/− charge state model for V_{As} in GaAs, and the potential contribution of this defect to the implant isolation process is discussed.

DOI: 10.1103/PhysRevB.77.235210 PACS number(s): 71.55.Eq, 72.80.Ey

I. INTRODUCTION

III-V compound semiconductors are currently employed in the fabrication of optoelectronic devices and high-frequency integrated circuits (ICs). Concerning III-V and more specifically GaAs processing technology, ion implantation plays a key role, presenting two major applications: semiconductor doping and electrical isolation.[1,2] In the latter application, also called implant isolation, irradiation with appropriate ion doses is used to convert a conductive layer into a highly resistive one[3] or to improve the isolation between neighbor devices in ICs. In order to achieve higher depths at energies provided by industrial implanters, light ions such as protons are often employed for implant isolation. Proton irradiation has been successfully used to isolate GaAs field effect transistors, high electron mobility transistors, and heterojunction bipolar transistors.[4] Waveguiding regions in optoelectronic devices were also fabricated using proton bombardment.[5]

The resistivity increase in the implant isolation process is attributed to the introduction of deep level defects, which can act both as compensating centers, reducing the total free-carrier concentration, or/and as scattering centers, reducing carrier mobility.[1,2] Understanding the defects introduced by the implantation and, in particular, characterizing deep levels associated with them are key points to achieve a proper description and optimization for this process step. Information concerning the charge state transition for each deep level is especially important[6] to predict if the corresponding defect can act as a compensating center and if it is a Coulombic or neutral scattering center, for example.

Concerning the particular case of GaAs, the deep levels introduced by proton bombardment has been previously studied by deep level transient spectroscopy (DLTS).[7,8] In *n*-type material, contributions similar to those obtained by electron irradiation were found. The two major peaks in the spectrum were identified[8] as E1 and E2. These levels are believed to be associated to As vacancies[9] and are good candidates to play an important role in the isolation process not only because of their high introduction rate[8] but also because of their characteristic annealing step at ~500 K,[10] which was observed for the isolation process.[11,12] Two different models were proposed to describe E1 and E2 charge state transitions,[9,13] but more data are still needed in order to confirm or reject any of them. In this paper, we have studied E1 and E2 emission rate behavior as a function of the electric field in an attempt to obtain further information on the charge state transition associated with each of these levels.

II. EXPERIMENTAL PROCEDURE

The GaAs samples are n/n^+ with a 3-μm-thick Si-doped ($n=3\times10^{16}$ cm^{-3}, measured by *C-V*) epitaxial layer grown by metal-organic chemical vapor deposition on a n^+ GaAs substrate at the reactor of the Escola Politécnica da Universidade de São Paulo, Brazil. The implantation step was carried out at room temperature using 600 keV protons. This energy value was chosen in order to place the defect distribution peak in the n^+ substrate, leaving a uniform defect distribution in the epitaxial layer. The proton dose employed was 1×10^{11} cm^{-2} and, during irradiation, the samples were tilted 15° from the beam axis to minimize channeling effects. After implantation, 0.8-mm-diameter circular top Schottky contacts were created by Al deposition using resistive evaporation and a mechanical mask. Back Ohmic contacts were created by manual application of an InGa alloy. *I-V* measurements (not shown) confirmed the Schottky diode formation.

DLTS measurements were carried out using a computer controlled system with a 1 MHz Boonton capacitance meter and a temperature controlled helium cryostat. The dependence of the emission rate on the electric field was investigated employing a double pulse technique, like in the double correlation DLTS,[14] but keeping a constant temperature. A capacitance transient is first recorded using a reverse voltage V_r and a pulse voltage V_{p1}, see Fig. 1(a). This transient corresponds to the emission from traps spatially localized between the depths x_d-λ and x_1-λ, where x_d and x_1 are the depletion depths corresponding to V_r and V_{p1}, respectively, and $\lambda=\sqrt{2}L_D\sqrt{E_f-E_t/kT}$.[15] After this, a second transient is recorded using the same V_r and a pulse voltage $V_{p2}(|V_{p2}|>|V_{p1}|)$, Fig. 1(b), corresponding to the emission from levels in the region between x_d-λ and x_2-λ, where x_2 is the depletion depth at a bias voltage V_{p2}. These two transients are then subtracted giving the contribution related to traps filled in the first case but not in the second one, Fig. 1(c). For values of $|V_{p2}-V_{p1}|$ small enough, the emission occurs at an approxi-

 ©2008 The American Physical Society

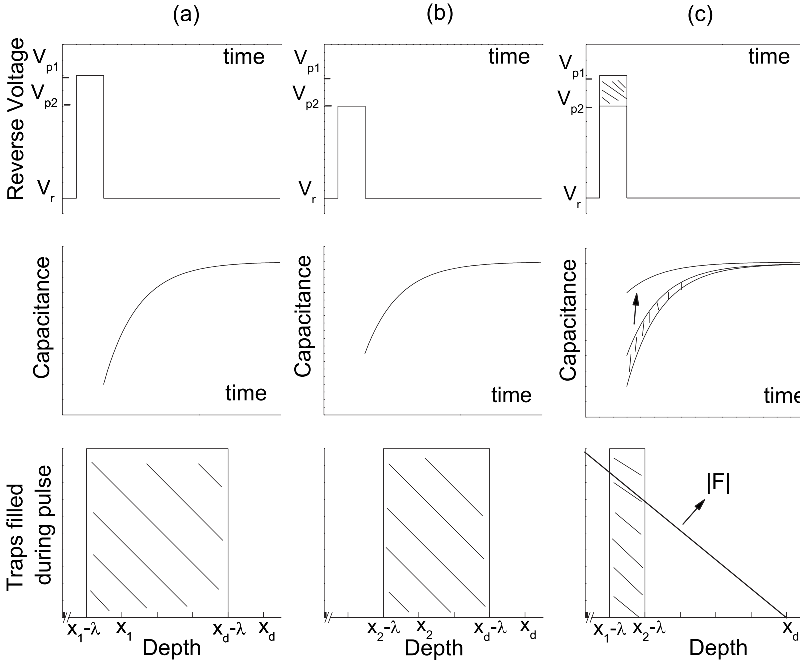

FIG. 1. Measurement scheme used to obtain information on the electron emission rate enhancement in an electric field. Column (a) presents a reverse bias pulse from V_r to V_{p1}, the corresponding capacitance transient and the traps filled during this pulse. Column (b) corresponds to the case of a pulse from V_r to V_{p2} and column (c) presents the results obtained for the subtraction $(a)-(b)$.

mately constant electric field. The rate can be extracted by a fitting procedure on the subtracted transient. In order to sweep the electric-field value, one can change the values of V_r, V_{p1}, and V_{p2}. Instead of keeping V_r fixed and change V_{p1} and V_{p2}, we preferred to keep both V_{p1} and V_{p2} fixed and vary V_r. By doing this, the spatial region actually being measured is kept the same. To guarantee a good signal-to-noise ratio, every transient was accumulated several hundred times.

III. MODELS FOR ELECTRON EMISSION RATE DEPENDENCE ON THE ELECTRIC FIELD

The electric-field influence on the electron emission rate from a deep level, e_n, can bring relevant information about the potential-well structure around the defect.[16] Three mechanisms are believed[17,18] to be responsible for this influence: direct tunneling,[19] Poole-Frenkel effect,[20] and phonon-assisted tunneling.[21–24] The first one is predominant at very high electric fields ($F > 10^7$ V/cm, a value much higher than the ones observed in this work).[17] In the Poole-Frenkel mechanism, the emission rate enhancement due to the electric field is attributed to a reduction of ΔE_t in trap ionization energy E_t.[20] This reduction is stronger for long-range potentials and weaker for short-range ones. Considering a Coulombic potential, ΔE_t is dependent on the charge of the defect, being null for a neutral center. For a one-dimensional Coulombic well,[17,18]

$$\Delta E_t = q\sqrt{\frac{ZqF}{\pi\varepsilon_r\varepsilon_0}}, \quad (1)$$

and

$$e_n = e_{n0}e^{\Delta E_t/k_BT}, \quad (2)$$

where q is the electron charge, ε_r is the semiconductor relative dielectric constant, e_{n0} is the deep level emission rate at null electric field, and Z is the empty defect charge. A linear $(F)^{1/2}\times\ln(e_n)$ plot is usually employed as a signature for the Poole-Frenkel effect in a Coulombic well.[25]

In the case of phonon-assisted tunneling, the trapped electron can absorb phonons and tunnel through the barrier at a higher energy, reducing both the barrier height and width and increasing the tunneling probability. Different models were used to describe this process. Here we will consider two of them: the one proposed by Pons and Makram-Ebeid[21] and the one presented by Karpus and Perel.[23,24]

According to the description of Pons and Makram-Ebeid, the total ionization rate is given by

$$e_n = e_{n0} + e_f,$$

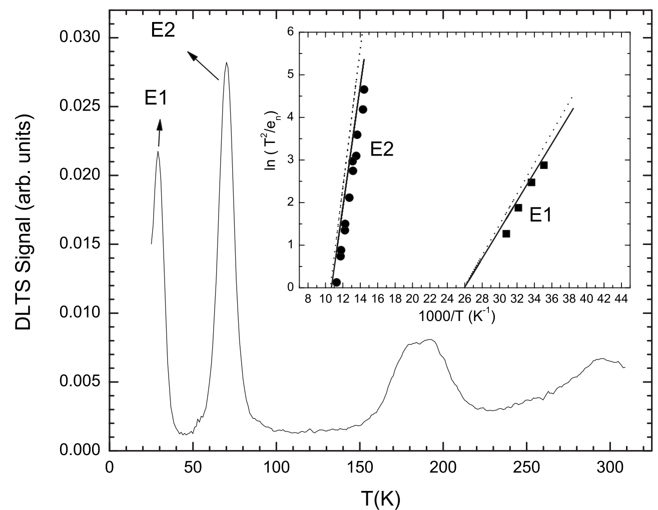

FIG. 2. DLTS spectrum of proton implanted n-type GaAs showing the peaks E1 and E2 (data obtained with a 50 s^{-1} rate window). The inset shows the Arrhenius plot for these two levels comparing them with previous proton implanted results (full lines) and electron irradiated results (dotted lines).

$$e_f = \sum_p \Pi_p \Gamma(\Delta_p), \qquad (3)$$

where e_f is the phonon-assisted tunneling ionization rate, Π_p is the occupation probability of a quasi level with an energy $p\hbar\omega$ higher than the trap energy, $\hbar\omega$ is the phonon energy, and $\Gamma(\Delta_p)$ is the tunneling ionization rate at the quasi level.

$\Gamma(\Delta)$ was calculated by Korol[19] considering a delta function potential well,

$$\Gamma(\Delta) = \gamma \frac{\Delta}{qK} e^{-K},$$

$$K = \frac{4\sqrt{2m^*}}{3\hbar F}\Delta^{3/2}, \qquad (4)$$

where γ is usually used as a fitting parameter, Δ is the barrier height, and m^* is the electron effective mass.

The occupation probability Π_p is given by[21]

$$\Pi_p = (1 - e^{-\hbar\omega/k_BT}) \sum_{n=0}^{\infty} e^{-n\hbar\omega/k_BT} J_p^2[2\sqrt{S(n+1/2)}], \qquad (5)$$

where J_p is a Bessel function of the first kind, T is the temperature, and S is the Huang-Rhys factor.[26]

The phonon-assisted tunneling theory presented by Karpus and Perel is based on the description of Abakumov *et al.*[27] to multiphonon capture and/or emission process in deep levels. They considered the introduction of the electric field on this description, yielding an analytical solution for the electron emission rate in the form

$$e_n = e_{n0} e^{F^2/F_c^2}, \qquad (6)$$

where the critical electric field, F_c, is given by

$$F_c = \sqrt{\frac{2m^*\hbar}{q^2\tau_2^3}}, \qquad (7)$$

and τ_2 is the temperature dependent tunneling time.[24] We will employ these models in order to describe the electron emission enhancement with the electric field for two levels in proton bombarded n-type GaAs.

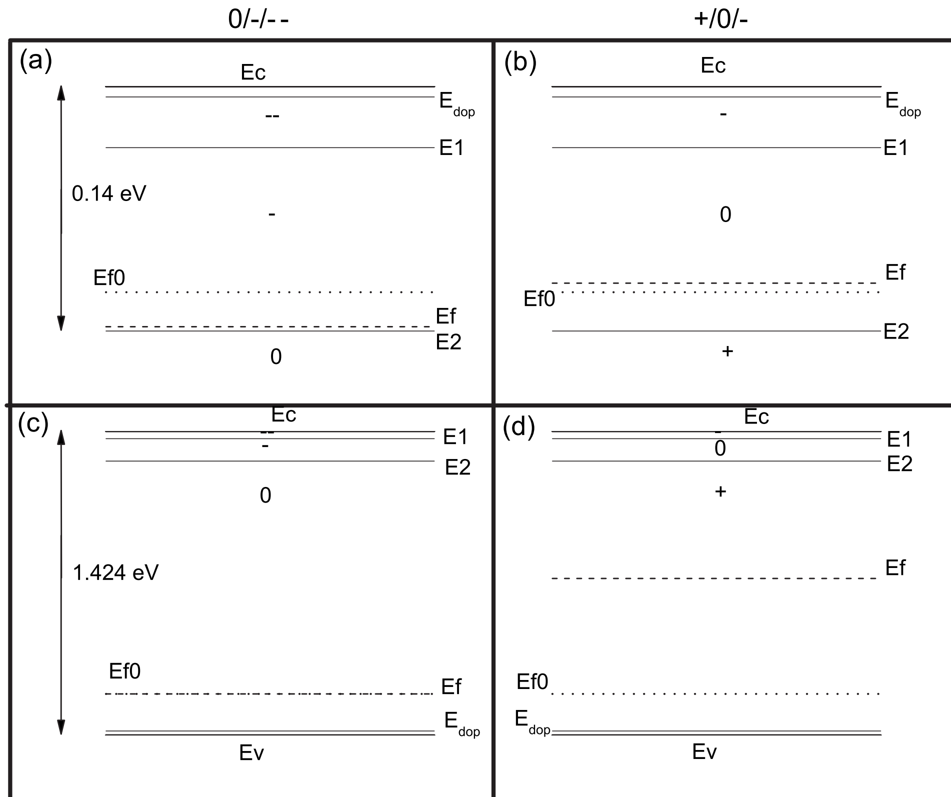

FIG. 3. Influence of the levels E1 and E2 on the Fermi-level position calculated using a simple charge neutrality model (Ref. 6) considering two proposed charge models (Refs. 9 and 13). The concentration of E1 and E2 used in the calculation was 1×10^{16} cm^{-3}. Cases (a) and (b) correspond to n-type GaAs with doping level at $E_c-0.006$ eV and a concentration of 1×10^{16} cm^{-3}. The Fermi level calculated without E1 and E2 is $E_{f0}=E_v+1.306$ eV and the corresponding free-electron concentration is $n0=9.9\times10^{15}$ cm^{-3}. Cases (b) and (c) consider p-type GaAs with doping level at $E_v+0.02$ eV and using the same concentration value (1×10^{16} cm^{-3}). For these cases, $E_{f0}=E_v+0.194$ eV and $p_0=9.99\times10^{15}$ cm^{-3}. In (a), using the model 0/−/−−, the introduction of E1 and E2 reduces the free-electron concentration to $n=4.6\times10^{15}$ cm^{-3} ($E_f=E_v+1.287$ eV). In (b), model +/0/−, n is increased to 1.2×10^{16} cm^{-3} ($E_f=E_v+1.311$ eV). Case (c), considering 0/−/−−, presents no modification in the free hole concentration ($p=p0$), but case (d), using +/0/−, reduces p to a value ($\sim8\times10^{6}$ cm^{-3}, $E_f=E_v+0.7344$ eV) close to the intrinsic one, corresponding to a very strong compensation.

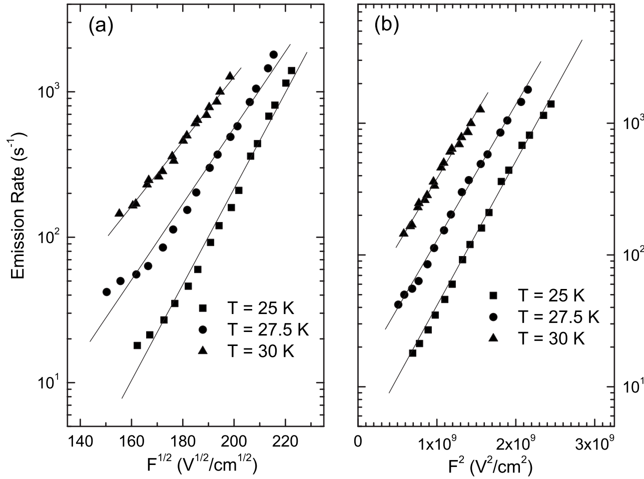

FIG. 4. Tentative description of E1 measured data with two models: (a) Poole-Frenkel and (b) Karpus and Perel phonon-assisted tunneling. The straight lines point out a positive identification for the case of the phonon-assisted tunneling model.

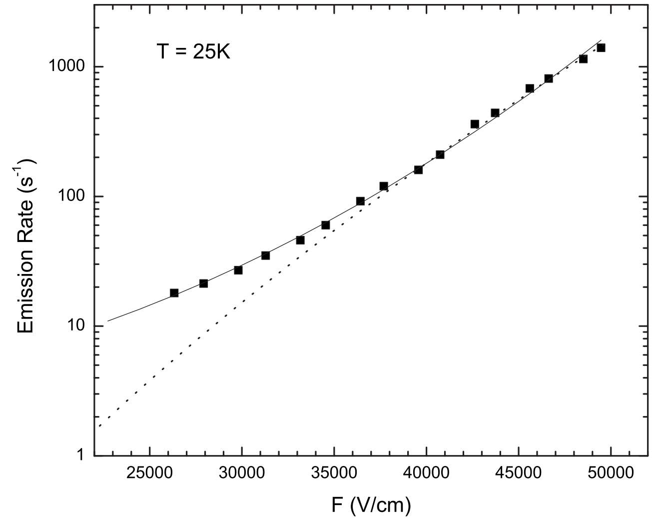

FIG. 5. Comparison of the measured data (points) with different fittings (lines) for E1. The full line corresponds to a fitting using the Karpus and Perel model for the phonon-assisted tunneling. The fitting parameters used were $e_{n0}=2.88\ s^{-1}$ and $F_c=19671.9$ V/cm. The dotted line corresponds to a Poole Frenkel fitting with $Z=1$ and $e_{n0}=1E\text{-}6\ s^{-1}$.

IV. RESULTS and DISCUSSION

Figure 2 presents the measured DLTS spectrum. The reverse voltage, pulse voltage, and pulse width values used were, respectively, −4.5 V, −4 V, and 0.1 ms. Two major peaks, E1 and E2, are observed at low temperatures together with other less pronounced contributions. The obtained apparent energies and cross sections, calculated from Arrhenius-plot linear fittings, are $E_{na}=0.035$ eV and $\sigma_{na}=3\times10^{-16}$ cm^2 for E1 and $E_{na}=0.14$ eV and $\sigma_{na}=4\times10^{-13}$ cm^2 for E2. These values are in good agreement with previous work on proton bombarded GaAs (Ref. 8) and also with electron irradiated data.[28,29] These levels are believed to be related to the same defect, V_{As}.[9] Two charge state transition schemes were tentatively associated with them: $0/-/--$ (Ref. 9) ($E2\Rightarrow0/-$ and $E1\Rightarrow-/--$) and $+/0/-$ (Ref. 13) ($E2\Rightarrow+/0$ and $E1\Rightarrow0/-$). Using the apparent energies and these transitions in a simple charge neutrality calculation based on Fermi statistics (see Ref. 6), one can realize that, in the first scheme, this defect is only able to act as a not too efficient compensating center in n-type GaAs, while, in the second scheme, it will act as a very good compensating center in p-type GaAs—see Fig. 3. The proper determination of the charge state transitions for these levels is then a key point to understand the possible contributions of this defect in the implant isolation process.

For the case of E1, measurements were performed at three different temperatures: 25, 27.5, and 30 K. The plot of the logarithm of this emission rate as a function of the square root of the electric field, Fig. 4(a), was not able to produce straight-line results, indicating that this enhancement is not well described by a Coulombic barrier Poole-Frenkel process alone. As also illustrated in Fig. 5, this model fails to reproduce the low-field region of the curve. However, it is in this region that the Poole-Frenkel enhancement is stronger and believed to be predominant,[25] which suggests the absence of this mechanism in the description of the electric-field dependent emission rate for E1. This suggestion is confirmed by the data in Fig. 4(b), where the logarithm of the emission rate is plotted as a function of the square of the electric field. The straight lines obtained reveal that the enhancement process can be completely describe by a plot in the form of Eq. (6), pointing to the phonon-assisted tunneling process as being responsible for the variation of the electron emission rate with the electric field for E1 in all measured electric fields and temperatures. Figure 5 compares the experimental data with two different fitting lines: the full line (better fitted) corresponds to the Karpus and Perel phonon-assisted tunneling model and the dotted line corresponds to the Poole-Frenkel model.

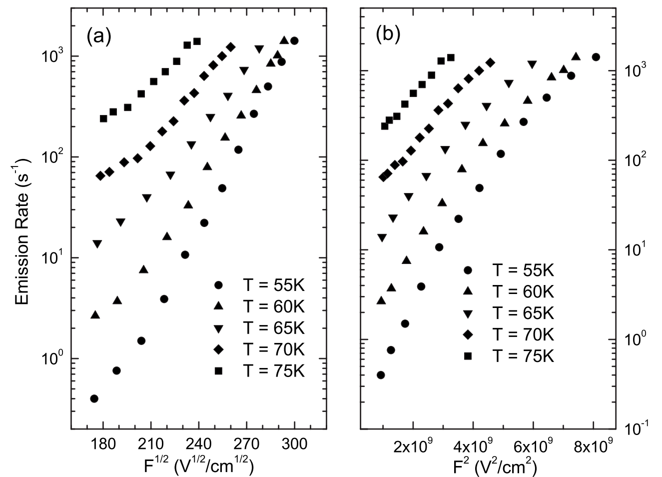

FIG. 6. Tentative description of E2 measured data with two models: (a) Poole-Frenkel and (b) Karpus and Perel phonon-assisted tunneling. The straight lines are not obtained in the figures, revealing that none of these models can describe experimental data alone.

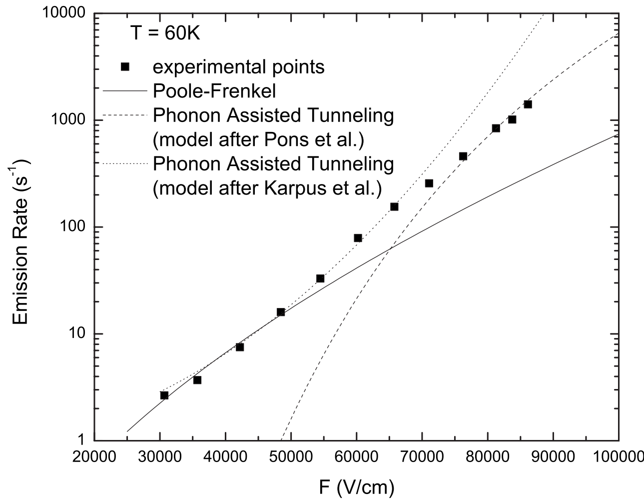

FIG. 7. Comparison of the measured data (points) with different fittings (lines). The dotted line corresponds to a fitting using the Karpus and Perel model for the phonon-assisted tunneling. The fitting parameters used were $e_{n0}=1\ \text{s}^{-1}$ and $F_c=29\,000\ \text{V/cm}$. The full line corresponds to a Poole-Frenkel fitting with $e_{n0}=0.01\ \text{s}^{-1}$ and the dashed line represents the phonon-assisted tunneling theory described by Pons with $E_t=0.14\ \text{eV}$, $\hbar\omega=0.01\ \text{eV}$, $S=0.8$, and $\gamma=2E\text{-}6\ \text{eV}^{-1}\ \text{s}^{-1}$.

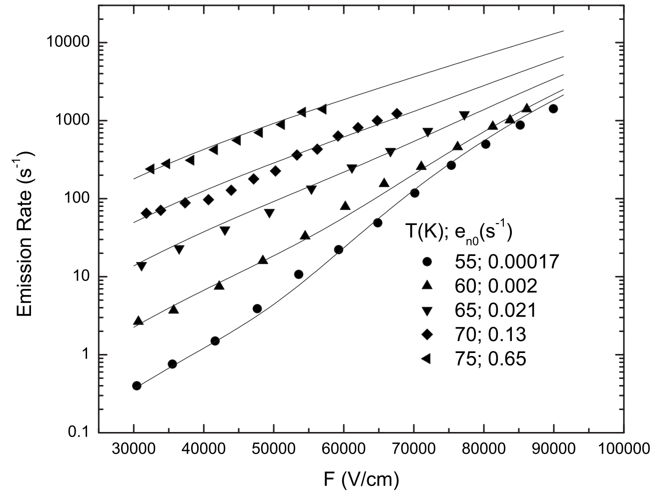

FIG. 8. E2 enhanced emission data fitting using the sum of a Poole-Frenkel term and a phonon-assisted tunneling one. Good fitting results are obtained using parameters values: $Z=1$, $S=0.8$, $\gamma=1.5\times10^{-6}\ \text{eV}^{-1}\ \text{s}^{-1}$, and $\hbar\omega=0.01\ \text{eV}$.

For the case of E2, the evolution of the electron emission rate with the electric field was measured at five different temperatures: 55, 60, 65, 70, and 75 K. Figure 6(a) presents the behavior of the logarithmic emission rate as a function of the square root of the electric field. It was not possible to fit data in all five temperatures with linear plots, indicating that the enhancement is not exclusively due to a Poole-Frenkel process. Plotting the same data as a function of the square of the electric field, it is not possible to fit the data at all temperatures with straight lines, revealing that all the enhancement also cannot be explained in terms of Eq. (6), representing the Karpus and Perel phonon-assisted tunneling formulation. In fact, as illustrated in Fig. 7, none of the models considered here could reproduce all experimental data by itself. However, as also depicted in this figure, the Poole-Frenkel effect describes well the low-field part of experimental points, while the Pons and Makram-Ebeid phonon-assisted tunneling model describes the high-field region. In order to properly reproduce the measured points, these two contributions were considered. We suggest a mixed model in which e_n is considered as the sum of the Poole-Frenkel contribution, Eq. (2), and the phonon-assisted tunneling ionization rate given by Pons and Makram-Ebeid,[21] Eq. (3), leading to a total description in the form of

$$e_n = e_{n0}e^{\Delta E_t/k_BT} + \sum_p \Pi_p \Gamma(\Delta_p). \tag{8}$$

Figure 8 illustrates the obtained curves. The values used for the parameters in the tunneling term were $\hbar\omega=10\ \text{meV}$ [corresponding to the peak of density of state for the T.A. mode in GaAs (Ref. 21)], $S=0.8$ and $\gamma=1.5\times10^{-6}\ \text{eV}^{-1}\ \text{s}^{-1}$. The zero-field-emission rate was also used as a fitting parameter.

V. CONCLUSIONS

Both levels E1 and E2 suffered a strong enhancement in their electron emission rates as a function of the increasing electric field. The behavior observed for E1 could be completely described by the phonon-assisted tunneling theory of Karpus and Perel without the participation of the Poole-Frenkel process, indicating the absence of a long-range attractive Coulombic tail in the potential imposed to the trapped electron. This is the case, for example, for a deltalike potential zero charged center. On the other hand, the e_n field enhancement measured for E2 could only be described by a combination of Poole-Frenkel and phonon-assisted tunneling processes. The inclusion of the Poole-Frenkel part is a signature for the presence of a Coulombic tail in a positively charged center.

Considering the previous association between proton bombarded and electron irradiated levels E1/E2 and the models suggested for these levels, data presented here are in very good agreement with the $+/0/-$ scheme and rejects the $0/-/--$ one, where, for example, the emission enhancement of E2 should be characteristic of a zero charged potential center, without any Coulombic tail Poole-Frenkel-type contribution. Within the scope of the models proposed for E1 and E2, these charge state transitions ($+/0$ for E2 and $0/-$ for E1) place V_{As} as an important component of the implant isolation scenario.

ACKNOWLEDGMENTS

This work was partially supported by Conselho Nacional de Desenvolvimento Científico e Tecnológico (CNPq) and by Fundação de Amparo à Pesquisa do Estado do Rio Grande do Sul (FAPERGS).

*Corresponding author; artur.coelho@gmail.com

[1] S. J. Pearton, Mater. Sci. Rep. **4**, 313 (1990).
[2] S. J. Pearton, Int. J. Mod. Phys. B **7**, 4687 (1993).
[3] J. P. de Souza, I. Danilov, and H. Boudinov, Appl. Phys. Lett. **68**, 535 (1996).
[4] D. V. Morgan and F. H. Eisen, *Gallium Arsenide Materials, Devices, and Circuits* (Wiley, New York, 1985), p. 161.
[5] T. C. Huang, Y. Chung, L. A. Coldren, and N. Dagli, IEEE J. Quantum Electron. **29**, 1131 (1993).
[6] A. V. P. Coelho and H. Boudinov, Nucl. Instrum. Methods Phys. Res. B **245**, 435 (2006).
[7] H. Boudinov, A. V. P. Coelho, H. H. Tan, and C. Jagadish, J. Appl. Phys. **93**, 3234 (2003).
[8] S. A. Goodman, F. D. Auret, M. Ridgway, and G. Myburg, Nucl. Instrum. Methods Phys. Res. B **148**, 446 (1999).
[9] J. C. Bourgoin, H. J. Von Bardeleben, and D. Stiévenard, J. Appl. Phys. **64**, R65 (1988).
[10] D. Pons, A. Mircea, and J. C. Bourgoin, J. Appl. Phys. **51**, 4150 (1980).
[11] H. Boudinov, A. V. P. Coelho, and J. P. de Souza, J. Appl. Phys. **91**, 6585 (2002).
[12] J. P. de Souza, I. Danilov, and H. Boudinov, J. Appl. Phys. **81**, 650 (1997).
[13] K. Saarinen, A. P. Seitsonen, P. Hautojarvi, and C. Corbel, Phys. Rev. B **52**, 10932 (1995).
[14] H. Lefevre and M. Schultz, Appl. Phys. **12**, 45 (1977).
[15] P. Blood and J. W. Orton, *The Electrical Characterization of Semiconductors: Majority Carriers and Electron States* (Academic, London, 1997).
[16] J. Bourgoin and M. Lanoo, *Point Defects in Semiconductors II, Experimental Aspects* (Springer, New York, 1983).
[17] P. A. Martin, B. G. Streetman, and K. Hess, J. Appl. Phys. **52**, 7409 (1981).
[18] G. Vincent, A. Chantre, and D. Bois, J. Appl. Phys. **50**, 5484 (1979).
[19] E. N. Korol, Sov. Phys. Solid State **19**, 1327 (1977).
[20] J. Frenkel, Phys. Rev. **54**, 647 (1938).
[21] D. Pons and S. Makram-Ebeid, J. Phys. (Paris) **40**, 1161 (1979).
[22] V. Karpus and V. I. Perel, JETP Lett. **42**, 497 (1985).
[23] V. Karpus and V. I. Perel, Zh. Eksp. Teor. Fiz. **91**, 2319 (1986)[Sov. Phys. JETP **64**, 1376 (1986)].
[24] S. D. Ganichev and W. Pretti, Phys. Solid State **39**, 1703 (1997).
[25] S. D. Ganichev, E. Ziemann, I. N. Yassievich, W. Prettl, A. A. Istratov, and E. R. Weber, Phys. Rev. B **61**, 10361 (2000).
[26] K. Huang and A. Rhys, Proc. R. Soc. London, Ser. A **204**, 406 (1950).
[27] V. N. Abakumov, I. A. Merkulov, V. I. Perel, and I. N. Yassievich, Zh. Eksp. Teor. Fiz. **89**, 1472 (1985) [Sov. Phys. JETP **62**, 853 (1985)].
[28] S. A. Goodman, F. D. Auret, and W. E. Meyer, Nucl. Instrum. Methods Phys. Res. B **90**, 349 (1994).
[29] D. Pons and J. C. Bourgoin, J. Phys. C **18**, 3839 (1985).